General Rogue waves and their dynamics in several reverse time integrable nonlocal nonlinear equations

Bo Yang[1,2] and Yong Chen[1,2,3,a)]
[1)] *Shanghai Key Laboratory of Trustworthy Computing, East China Normal University, Shanghai, 200062, People's Republic of China*
[2)] *MOE International Joint Lab of Trustworthy Software, East China Normal University, Shanghai, 200062, People's Republic of China*
[3)] *Department of Physics, Zhejiang Normal University, Jinhua, 321004, China*

A study of general rogue waves in some integrable reverse time nonlocal nonlinear equations is presented. Specifically, the reverse time nonlocal nonlinear Schrödinger (NLS) and nonlocal Davey-Stewartson (DS) equations are investigated, which are nonlocal reductions from the AKNS hierarchy. By using Darboux transformation (DT) method, several types of rogue waves are constructed. Especially, a unified binary DT is found for this nonlocal DS system, thus the solution formulas for nonlocal DSI and DSII equation can be written in an uniform expression. Dynamics of these rogue waves is separately explored. It is shown that the (1+1)-dimensional rogue waves in nonlocal NLS equation can be bounded for both x and t, or develop collapsing singularities. It is also shown that the (1+2)-dimensional line rogue waves in the nonlocal DS equations can be bounded for all space and time, or have finite-time blowing-ups. All these types depend on the values of free parameters introduced in the solution. In addition, the dynamics patterns in the multi- and higher-order rogue waves exhibits more richer structures, most of which have no counterparts in the corresponding local nonlinear equations.

Keywords: Reverse time nonlocal nonlinear equations, Darboux transformation, Rogue waves

I. INTRODUCTION

The integrable nonlinear evolution equations are exactly solvable models which play an important role in the field of nonlinear science, especially in the study of nonlinear physical systems, including nonlinear optics, Bose-Einstein condensates, plasma physics and ocean water waves. Most of these integrable equations are local equations, that is, the solutions evolution only depends on the local solution value. In recent years, numbers of new integrable nonlocal equations were proposed and studied[1–20]. The first such nonlocal equation was the $\mathcal{PT}$-symmetric nonlocal nonlinear Schrödinger (NLS) equation[1]:

$$\mathrm{i}q_t(x,t) = q_{xx}(x,t) + 2\sigma q^2(x,t)q^*(-x,t). \tag{1}$$

Here, $\sigma = \pm 1$ is the sign of nonlinearity (with the plus sign being the focusing case and minus sign the defocusing case), and the asterisk * represents complex conjugation. It is noted that $\mathcal{PT}$-symmetric systems have attracted a lot of attention in optics and other physical fields in recent years[21–25].

Following this nonlocal $\mathcal{PT}$-symmetric NLS equation, some new reverse space-time and reverse time type nonlocal nonlinear integrable equations were also introduced and quickly reported[6–8]. They are integrable infinite dimensional Hamiltonian dynamical systems, which arise from remarkably simple symmetry reductions of general ZS-AKNS scattering problems where the nonlocality appears in both space and time or time alone. These examples including the reverse space-time and/or the reverse time only nonlocal NLS[6], the

[a)]Electronic mail: (Corresponding author.) ychen@sei.ecnu.edu.cn.

(complex) modified Korteweg-deVries, sine-Gordon, three-wave interactions, derivative NLS (dNLS), Davey-Stewartson, discrete NLS type[6], Sasa-Satsuma[7](S-S) and nonlocal complex short pulse[8](CSP) equations , and many others[8].

These nonlocal equations, because of their novel space and/or time coupling, are distinctly different from local equations. Indeed, solution properties in some of these nonlocal equations have been analyzed by the inverse scattering transform method, Darboux transformation or the bilinear method. On the one hand, those new systems could reproduce solution patterns which already have been discovered in their local counterparts. On the other hand, some interesting behaviors such as blowing-up solutions with finite-time singularities[8,15] and the existence of even more richer structures have also been revealed[7,14–16]. Although these nonlocal equations are mathematically interesting. In the view of further potential applications, it links to an unconventional system of magnetics[23], and relates to the concept of $\mathcal{PT}$-symmetry, which is a hot research area in contemporary physics[22].

Rogue waves have attracted a lot of attention in recent years due to their dramatic and often damaging effects, such as in the ocean and optical fibers[26,27]. The first analytical expression of a rogue wave for the NLS equation was derived by Peregrine in 1983[28]. Later, the analytical rogue-wave solutions have been derived and interesting dynamical patterns been revealed for a large number of integrable systems[29–52].

As an unexplored and interesting subject, rogue waves in the nonlocal integrable systems have received much attention. For local integrable equations, the evolution for most rogue-wave solutions depends only on the local solution value with its local space and time derivatives. However, for the nonlocal equations, the sates of rogue-wave solutions at distinct locations x and $-x$ are directly related[14,15,20]. Hence, these facts are basically important and further motivate us ask an interesting open question: If one only consider the connections between the sates of rogue-wave solutions at reverse time points t and $-t$, whether there are rogue waves existing in some reverse time nonlocal nonlinear equations?

In this article, to give an answer to this question, we study rogue waves in several reverse time integrable nonlocal nonlinear equations. As typically concrete examples, we focus on the reverse time nonlocal NLS equation:

$$\mathrm{i}q_t(x,t) = q_{xx}(x,t) + 2\sigma q^2(x,t)q(x,-t), \tag{2}$$

and the reverse time nonlocal DS equations:

$$iq_t + \frac{1}{2}\gamma^2 q_{xx} + \frac{1}{2}q_{yy} + (qr - \phi)q = 0, \tag{3}$$

$$\phi_{xx} - \gamma^2\phi_{yy} - 2\left(qr\right)_{xx} = 0, \tag{4}$$

where $r(x,y,t) = \sigma q(x,y,-t)$, q, r and ϕ are functions of x, y, t, $\gamma^2 = \pm 1$ is the equation-type parameter (with $\gamma^2 = 1$ being the DS-I and $\gamma^2 = -1$ being DS-II). With certain reductions, Eq.(2) and Eqs.(3)-(4) can be derived from the member of the (1+1)- and (1+2)-dimensional AKNS hierarchy, respectively.

By using Darboux transformation method, we derive general rogue waves for these three nonlocal equations, solution formulas are given under certain reductions of wave functions and adjoint wave functions. More interestingly and coincidentally, we find a unified binary DT for this nonlocal DS system, so that rogue-wave solutions in nonlocal DSI and DSII equation can be expressed in a unified form, which is quite different from the constrictions of DT in the local DS[60] and partially $\mathcal{PT}$-symmetric DS equations[15]. In addition, dynamics of these rogue waves is further analyzed. For these reverse time nonlocal equations, it is shown that general rogue waves can be bounded for all space and time. More importantly, they can also develop collapsing singularities (for nonlocal NLS) or finite time blowing-ups (for nonlocal DS), which have no counterparts for the local equations. In addition, under certain parameter conditions, the dynamics of multi-rogue waves and higher-order rogue waves can exhibit more patterns. Most of them haven't been found before in the integrable nonlocal nonlinear equations.

II. ROGUE WAVES IN THE REVERSE TIME NONLOCAL NONLINEAR SCHRÖDINGER EQUATION

In this section, we consider rogue waves in the focusing reverse time nonlocal NLS equation (2) (with $\sigma = 1$), which approach the unit constant background when $x, t \to \pm\infty$. In the local NLS equation, general rogue waves in the form of rational solutions have been reported in[30–35], which are bounded solutions for both t and x. For the nonlocal NLS equation (1), we will show that the reverse time nonlocal NLS equation admits a wider variety of rogue waves. In addition to the non-collapsing patterns, there are also other types of rogue waves which can develop collapsing singularities.

It has been pointed that Eq.(2) is an integrable Hamilton evolution equation that admits an infinite number of conservation laws[6]. The first four conserved quantities are verified and given by

$$\begin{aligned}
I_1 &= \int_{-\infty}^{\infty} q(x,t)q(x,-t)dx, \\
I_2 &= \int_{-\infty}^{\infty} q(x,-t)q_x(x,t)dx, \\
I_3 &= \int_{-\infty}^{\infty} \left[q(x,-t)q_{xx}(x,t) + q^2(x,t)q^2(x,-t)\right] dx, \\
I_4 &= \int_{-\infty}^{\infty} q(x,-t)\left\{q_{xxx}(x,t) + [q^2(x,t)q(x,-t)]_x \right. \\
&\qquad \left. + 2q(x,-t)q(x,t)q_x(x,t)\right\} dx.
\end{aligned}$$

For this equation, the evolution at time t depends on not only the local solution at t, but also the nonlocal solution at the reverse time point $-t$. That is, solution states at reverse time points t and $-t$ are directly related. Especially, N-solitons are derived recently[53] via the Riemann-Hilbert solutions of AKNS hierarchy under the reverse-time nonlocal reduction. In this part, we focus on the general rogue waves.

We begin with the following ZS-AKNS scattering problem[54,55]:

$$\Phi_x = U(q,r,\lambda)\Phi, \tag{5}$$
$$\Phi_t = V(q,r,\lambda)\Phi, \tag{6}$$

where Φ is a column-vector,

$$U(q,r,\lambda) = -\mathrm{i}\lambda\sigma_3 + Q, \tag{7}$$
$$V(q,r,\lambda) = 2\mathrm{i}\lambda^2\sigma_3 - 2\lambda Q - \mathrm{i}\sigma_3\left(Q_x - Q^2\right), \tag{8}$$
$$\sigma_3 = \mathrm{diag}(1,-1),\ Q(x,t) = \begin{pmatrix} 0 & q(x,t) \\ r(x,t) & 0 \end{pmatrix},\ x,t \in \mathbb{R}.$$

The compatibility condition of these equations give rise to the zero-curvature equation

$$U_t - V_x + [U,V] = 0, \tag{9}$$

which yields the following coupled system for potential functions (q,r) in the matrix $Q(x,t)$:

$$\mathrm{i}q_t = q_{xx} - 2q^2 r, \tag{10}$$
$$\mathrm{i}r_t = -r_{xx} + 2r^2 q. \tag{11}$$

The focusing reverse-time nonlocal NLS equation (2) is obtained from the above coupled system (10)-(11) under the symmetry reduction:

$$r(x,t) = -q(x,-t). \tag{12}$$

As it is stressed by Ablowitz and Musslimani[3]:“ This reduction is new, remarkably simple, which has not been noticed in the literature and leads to a nonlocal in time NLS hierarchy.” Under reduction (12), the potential matrix Q satisfies the following symmetry condition:

$$Q^T(x,t) = -Q(x,-t). \tag{13}$$

To construct the Darboux transformation, we need to introduce the adjoint-spectral problem for (5)-(6):

$$-\Psi_x = \Psi U(q, r, \zeta), \tag{14}$$
$$-\Psi_t = \Psi V(q, r, \zeta), \tag{15}$$

here Ψ is a row-vector.

A. N-fold Darboux transformation and reverse-time reduction

For the ZS-AKNS scattering problem, there is a general Darboux transformation proposed in[58,59], which can be represented as:

$$T = I + \frac{\zeta_1 - \lambda_1}{\lambda - \zeta_1} P_1,\ P_1 = \frac{\Phi_1 \Psi_1}{\Psi_1 \Phi_1}, \tag{16}$$

where $\Phi_1 = (\phi_1, \phi_2)^T$ is a solution with spectral parameter $\lambda = \lambda_1$, and $\Psi_1 = (\psi_1, \psi_2)^T$ is a solution of conjugation system with spectral parameter $\zeta = \zeta_1$. This DT can convert (5)-(6) into a new system

$$\left(\Phi_{[1]}\right)_x = U(q_{[1]}, r_{[1]}, \lambda)\Phi_{[1]},$$
$$\left(\Phi_{[1]}\right)_t = V(q_{[1]}, r_{[1]}, \lambda)\Phi_{[1]},$$

with the transformation between potential matrix:

$$Q_{[1]} = Q + \mathrm{i}(\zeta_1 - \lambda_1)\left[\sigma_3, P_1\right]. \tag{17}$$

Next, we consider the reduction of DT for system (5)-(6). Due to the potential symmetry (13), it is shown by direct calculation that matrix U satisfy the symmetry:

$$U^T(x, t, \lambda) = -U(x, -t, -\lambda). \tag{18}$$

For the given form (7) in matrix U, the matrix V which satisfies the zero-curvature equation (9) with the specific form of λ-dependence as in Eq. (8) is unique. Therefore, by utilizing symmetry (18) and the zero-curvature equation (9), we can derive the corresponding symmetry of the matrix V:

$$V^T(x, t, \lambda) = V(x, -t, -\lambda). \tag{19}$$

Using these U and V symmetries, we can derive the symmetries of wave functions Φ and adjoint wave functions Ψ, and hence the symmetry of the Darboux transformation for the reverse-time nonlocal NLS equation (1). Applying these symmetries to the spectral problems (5)-(6), we get

$$-\Phi_x^T(x, -t) = \Phi^T(x, -t)U(x, t, -\lambda), \tag{20}$$
$$-\Phi_t^T(x, -t) = \Phi^T(x, -t)V(x, t, -\lambda). \tag{21}$$

Thus, if $\Phi(x, t)$ is a wave function of the linear system (5)-(6) at λ, then $\Phi^T(x, -t)$ is an adjoint wave function of the adjoint system at $\zeta = -\lambda$. In this case, if $\Psi_1(x, t, \lambda)$ and $\Phi^T(x, -t, -\lambda)$ are linearly dependent on each other, then matrix (16) would preserve the potential reduction (12) and thus be a Darboux transformation for the reverse-time nonlocal NLS equation (1). Specifically, we have the following results.

Proposition 3.1. For any spectral $\lambda_1, \zeta_1 \in \mathbb{C}$, if

$$\zeta_1 = -\lambda_1,\ \Psi_1(x, t, \zeta_1) = \alpha\, \Phi_1^T(x, -t, \lambda_1), \tag{22}$$

where α is a complex constant. Then the Darboux matrix (16) accords with a Darboux transformation for the focusing reverse-time nonlocal NLS equation (1).

This proposition can be readily proved by checking that the new potential matrix $Q_{[1]}$ from Eq. (17) satisfies the symmetry (12) under conditions (22). Via a direct calculation, this property can be easily verified.

The N-fold Darboux transformation is a N times iteration of the elementary DT with corresponding reductions. For the local NLS equation, a N-fold Darboux matrix has been given in[57]. Here, with the reduction given above, we have the following N-fold Darboux matrix.

Proposition 3.2. *The N-fold Darboux transformation matrix for the focusing $\mathcal{PT}$-symmetric NLS equation can be represented as:*

$$T_N = I - YM^{-1}D^{-1}X, \tag{23}$$

where,

$$\begin{aligned}
&Y = [\ |y_1\rangle,\ |y_2\rangle, \ldots, |y_N\rangle\ ],\ |y_k\rangle = \Phi_k(\lambda_k),\\
&X = [\ \langle x_1|,\ \langle x_2|, \ldots, \langle x_N|\ ],\ \langle x_k| = \Psi_k(\zeta_k),\\
&M = \left(m_{i,j}^{(N)}\right)_{1\le i,j\le N},\ m_{i,j}^{(N)} = \frac{\langle x_i|y_j\rangle}{\lambda_j - \zeta_i},\\
&D = \mathrm{diag}\left(\lambda-\zeta_1, \lambda-\zeta_2, \ldots, \lambda-\zeta_N\right),
\end{aligned}$$

where $|y_i\rangle$ solves the spectral equation (5)-(6) at $\lambda = \lambda_i$, and $\langle x_j|$ solves the adjoint spectral equation (14)-(15) at $\zeta = \zeta_j$. Here, for any $k \in \mathbb{N}^+$, we should have $\zeta_k = -\lambda_k$ with$\langle x_k(x,t)| = |y_k(x,-t)\rangle^T$.

Moreover, the Bäcklund transformation between potential functions is:

$$u^{[N]} = u + 2\mathrm{i}\frac{\begin{vmatrix} M & X_2 \\ Y_1 & 0 \end{vmatrix}}{|M|}, \tag{24}$$

where Y_1 represents the first row of matrix Y, and X_2 represents the second column of matrix X.

Expression (24) can be found[56], which appears as Riemann-Hilbert solution. The proof of this theorem has already been given.[56,57]

B. Derivation of general rogue-wave solutions

In this section, we derive a general formula for rogue waves. First of all, we need the general eigenfunctions solved from the linear system (5)-(6) and its adjoint system (14)-(15). Choosing a plane wave solution $u_{[0]} = e^{-2\mathrm{i}t}$ to be the seed solution, we can derive a general wave function for the linear system (5)-(6) as

$$\Phi(x,t) = \mathcal{D}\phi(x,t), \tag{25}$$

where $\mathcal{D} = \mathrm{diag}\left(e^{-\mathrm{i}t}, e^{\mathrm{i}t}\right)$,

$$\begin{aligned}
&\phi(x,t) = \begin{pmatrix} c_1 e^{A} + c_2 e^{-A} \\ c_4 e^{A} + c_3 e^{-A} \end{pmatrix}, \\
&A = \sqrt{-\lambda^2-1}(x - 2\lambda t + \theta),\\
&c_3 = c_2\left(\mathrm{i}\lambda - \sqrt{-\lambda^2-1}\right),\ c_4 = c_1\left(\mathrm{i}\lambda + \sqrt{-\lambda^2-1}\right),
\end{aligned} \tag{26}$$

and c_1, c_2, θ are arbitrary complex constants. Imposing the conditions of λ being purely imaginary, i.e., $\lambda = ih$, $|\lambda| > 1$, θ is complex. Furthermore, to obtain the adjoint wave function, one can use symmetry condition (22). Through a simple Gauge transformation on the complex constant c_1, c_2, we can normalize $\alpha = 1$. Hence, the adjoint wave function to Eqs.(14)-(15) at $\zeta = -\lambda$ satisfying (22) can be given as:

$$\Psi(x,t,\zeta) = \psi(x,t,\zeta)\mathcal{D}^*, \tag{27}$$

where

$$\psi(x,t,\zeta) = \phi^T(x,-t,\lambda). \tag{28}$$

Moreover, with a constant normalization on free complex constants c_1 and c_2, the wave function $\phi(x,t)$ becomes

$$\phi(x,t,\lambda) = \frac{1}{\sqrt{h-1}} \begin{pmatrix} \sinh\left[A + \frac{1}{2}\ln\left(h+\sqrt{h^2-1}\right)\right] \\ \sinh\left[-A + \frac{1}{2}\ln\left(h+\sqrt{h^2-1}\right)\right] \end{pmatrix}. \tag{29}$$

Here, the scaling constant $\sqrt{h-1}$ is introduced so that this wave function does not approach zero in the limit of $h \to 1$ (i.e., $\lambda \to \mathrm{i}$). In the view of wave function and Proposition 3.2, this scaling of the wave function does not affect the solution except for a simple shifting $\frac{1}{2\sqrt{h^2-1}} \ln\left(|\frac{c_1}{c_2}|\right)$ occurs on the x-direction.

Next, to derive rogue-wave solutions from above wave functions and adjoint wave functions, we need to choose spectral parameters λ_k and ζ_k so that the exponents A can vanish under certain limits. Thus, we can take λ_k to be i, and correspondingly, ζ_k to be $-\mathrm{i}$. Specifically, we choose spectral parameters $\lambda = \lambda_k$, $\zeta = \zeta_k$ and complex parameters $\theta = \theta_k$, where

$$\lambda_k = \mathrm{i}(1+\epsilon_k^2), \quad \zeta_k = -\mathrm{i}(1+\epsilon_k^2), \tag{30}$$

$$\theta_k = \sum_{j=0}^{N-1} s_j \epsilon_k^{2j}, \quad 1 \le k \le N, \tag{31}$$

$s_0, s_1, \ldots, s_{n-1}$ are k-independent complex constants.

Thus, with $\lambda = \mathrm{i}(1+\epsilon^2), \zeta = -\mathrm{i}(1+\widetilde{\epsilon}^2)$, we have the following expansions:

$$\phi(x,t,\lambda) = \sum_{k=0}^{\infty} \phi^{(k)} \epsilon^{2k}, \ \psi(x,t,\zeta) = \sum_{k=0}^{\infty} \psi^{(k)} \widetilde{\epsilon}^{2k}, \tag{32}$$

$$\frac{\psi(x,t,\zeta)\phi(x,t,\lambda)}{\lambda-\zeta} = \sum_{k=0}^{\infty}\sum_{l=0}^{\infty} m_{k,l}\, \widetilde{\epsilon}^{2k} \epsilon^{2l}, \tag{33}$$

where

$$\phi^{(k)} = \lim_{\epsilon\to 0} \frac{\partial^{2k}\phi(x,t,\lambda)}{(2k)!\partial\epsilon^{2k}}, \quad \psi^{(k)} = \lim_{\epsilon\to 0} \frac{\partial^{2k}\phi^T(x,-t,\lambda)}{(2k)!\partial\epsilon^{2k}}, \tag{34}$$

$$m_{k,l} = \lim_{\epsilon,\widetilde{\epsilon}\to 0} \frac{1}{(2k-2)!(2l-2)!} \frac{\partial^{2k+2l-4}}{\partial\widetilde{\epsilon}^{2k-2}\partial\epsilon^{2l-2}} \left[\frac{\phi^T(-t,\zeta)\phi(t,\lambda)}{\lambda-\zeta}\right]. \tag{35}$$

Here, we use a different notation $\widetilde{\epsilon}$ instead of ϵ in the adjoint wave function ϕ for above expansions. In the sense of limit $\epsilon \to 0$, $\widetilde{\epsilon} \to 0$, they still meets the reduction condition (22). Therefore, applying these expansions to each matrix element in the Bäcklund transformation (24), performing simple determinant manipulations and taking the limits of $\epsilon_k, \widetilde{\epsilon}_k \to 0$ $(1 \le k \le N)$, we derive general rogue waves in the following Theorem.

Theorem 3.1. *The N-th order rogue waves in the focusing reverse-time nonlocal NLS equation can be formulated as:*

$$u_N(x,t) = e^{-2it}\left(1 + 2\mathrm{i}\frac{\tau_1}{\tau_0}\right), \tag{36}$$

where

$$\tau_0 = \det_{1\le i,j\le n}(m_{i,j}), \quad \tau_1 = \det\begin{pmatrix} (m_{i,j})_{1\le i,j\le N} & Y_{(2)} \\ X_{(1)} & 0 \end{pmatrix},$$

$$X=\left[\phi^{(0)},\phi^{(1)},...,\phi^{(N-1)}\right],\ Y=\left[\psi^{(0)},\psi^{(1)},...,\psi^{(N-1)}\right]^{T}.$$

Here, $X_{(1)}$ stands the 1-st row in matrix X, while $Y_{(2)}$ represents the 2-nd column in Y. Functions $\phi(\lambda)$ and $\psi(\zeta)$ are defined in the form as (28)-(29), the matrix element $m_{i,j}$ is given through limitation (35).

Since wave functions and adjoint wave functions in the Darboux transformation for the reverse-time nonlocal NLS equation (1) are related via the reverse-time reduction, this new reduction will lead to different types of rogue waves, which will be discussed in the following.

C. Dynamics in the rogue-wave solutions

In this section, we give a discussion on the dynamics of these rogue-wave solutions.

1. Fundamental rogue-wave solution

The first-order (fundamental) rogue wave is obtained by setting $N=1$ in Eq. (36), where the matrix elements can be obtained from Theorem 3.1. In this case,

$$\tau_0=m_{1,1}=-\frac{\mathrm{i}}{2}\left(8s_0x+4s_0^2+16t^2+4x^2+1\right),$$
$$\tau_1=\begin{vmatrix} m_{1,1} & Y_2\\ X_1 & 0\end{vmatrix}=\frac{1}{2}\left(8s_0x+4s_0^2+16t^2+8\mathrm{i}t+4x^2-1\right),$$

where s_0 is complex constants. Thus, the first-order rogue-wave is given by

$$\begin{aligned}u_1(x,t)&=e^{-2\mathbf{i}\,t}\left(1+2\,\mathrm{i}\frac{\tau_1}{\tau_0}\right)\\ &=-\frac{e^{-2\mathbf{i}t}\left(8s_0x+4s_0^2+16t^2+16\mathbf{i}t+4x^2-3\right)}{8s_0x+4s_0^2+16t^2+4x^2+1}.\end{aligned}$$

Denoting $x_0=\mathrm{Re}\,(s_0)$ and $y_0=\mathrm{Im}\,(s_0)$, this rogue wave can be rewritten as

$$u_1(x,t)=-e^{-2\mathbf{i}\,t}\left[1+\frac{4(4\mathrm{i}t-1)}{16t^2+4\,(\hat{x}+\mathrm{i}y_0)^{\,2}+1}\right],\tag{37}$$

where $\hat{x}=x+x_0$. Hence, this solution has one non-reducible real parameter y_0, since the parameter x_0 can be removed by space-shifting. Moreover, it is interesting to find that this fundamental rogue-wave solution also admits the first order rogue wave recently derived[20] in the $\mathcal{PT}$-symmetric nonlocal NLS equation. This is due to an important property which solution (37) satisfies:

$$u_1^*(-\hat{x},t)=u_1(\hat{x},-t)\tag{38}$$

For this rogue wave solution, when $y_0^2<1/4$, it is shown to be nonsingular. If $y_0=0$, it degenerates into the classical Peregrine soliton for the local NLS equation. [note that any solution of the local NLS equation satisfying $u^*(x,t)=u(x,-t)$ would satisfy the reverse-time nonlocal equation (1)]. The peak amplitude of this Peregrine soliton is 3, i.e., three times the level of the constant background. But if $y_0\neq 0$, its peak amplitude would accurately becomes $\left|\frac{4s_0^2+3}{4s_0^2-1}\right|$, which is higher than 3. One of such solutions is shown in Fig. 1.

However, once $y_0^2\geq 1/4$, this rogue wave would blow-up at $x=0$ with two time points $t_c=\pm\sqrt{(4y_0^2-1)/16}$. One such blowing-up solution is displayed in Fig.2. Since wave collapse has been reported in bright solitons[1,6] for the nonlocal NLS equation (1). Here we see that collapse occurs for rogue waves in the reverse-time nonlocal equation as well.

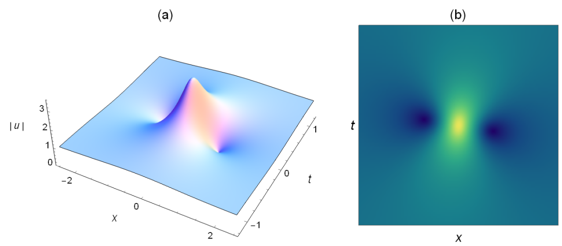

FIG. 1. The nonsingular first-order rogue wave solution (37). (a). $s_0 = r_0 = \frac{\mathrm{i}}{6}$(corresponding to $y_0 = 1/6$); (b) is the corresponding density plot.

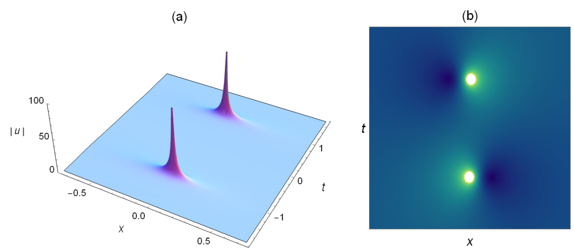

FIG. 2. A collapsing first-order rogue wave (37) with $s_0 = 2\mathrm{i}$; (a) 3D plot; (b) density plot.

2. Higher-order rogue-wave solution

Next, we consider the second order rogue waves, which are given in (36) with $N = 2$. In this case, the general second order rogue wave can be obtained as

$$q_2(x,t) = e^{-2\mathbf{i}\,t}\left(1 + 2\,\mathrm{i}\frac{\tau_1}{\tau_0}\right) \tag{39}$$

where,

$$\begin{aligned}
\tau_0 = -\frac{4}{9}\{&4096t^6 + 3072t^4x^2 + 768t^2x^4 + 64x^6 + 6912t^4 - 1152t^2x^2 + 1584t^2 + 48x^4\\
&+108x^2 + 384s_0^5x + 48s_0^4\left(16t^2 + 20x^2 + 1\right) + 64s_0^3\left[x\left(48t^2 + 20x^2 + 3\right) - 3s_1\right] + 64s_0^6\\
&-48s_1x\left(-48t^2 + 4x^2 - 3\right) + 12s_0^2\left[-48s_1x + 256t^4 + 96t^2\left(4x^2 - 1\right) + 80x^4 + 24x^2 + 9\right]\\
&+144s_1^2 + 24s_0\left[6s_1\left(16t^2 - 4x^2 + 1\right) + x\left(256t^4 + 128t^2x^2 + 16x^4 + 8x^2 - 96t^2 + 9\right)\right] + 9\},
\end{aligned}$$

$$\begin{aligned}
\tau_1 = &-\frac{8}{3}\left[1024t^5 + \mathrm{i}\left(1280t^4 + 16x^4 + 64s_0x^3 + 24x^2 + 96s_0^2x^2 + 48s_0x + 64s_0^3x + 48s_1x\right)\right.\\
&+\mathrm{i}t^2\left(384x^2 + 768s_0x + 384s_0^2 + 288\right) + t^3\left(512x^2 + 1024s_0x + 512s_0^2 + 128\right) + t\left(256s_0x^3 + 384s_0^2x^2\right.\\
&\left.\left.+256s_0^3x - 192s_0x + 192s_1x + 64s_0^4 - 96s_0^2 + 192s_0s_1 + 64x^4 - 96x^2 - 60\right) + \mathrm{i}\left(24s_0^2 + 16s_0^4 + 48s_0s_1 - 3\right)\right],
\end{aligned}$$

By choosing free complex parameters s_0 and s_1 in (39), we can get both nonsingular and singular (blowing-up) solutions. One nonsingular triangular pattern solution is observed and displayed in Fig. 3(a). Even though the present solution does not admit $u^*(x,t) = u(x,-t)$ and thus does not satisfy the local NLS equation, this pattern resemble that in the local NLS equation[30,32–35]. Moreover, this triangular pattern features the double temporal bumps with a single temporal bump, which is also different from the pattern found in the $\mathcal{PT}$-symmetric nonlocal NLS equation[20]. For the second-order rogue waves, the blowing-up solutions are shown to have more interesting and complex patterns, which have not been observed before. Five of them are displayed in Fig. 3. In panel (b), the solution contains

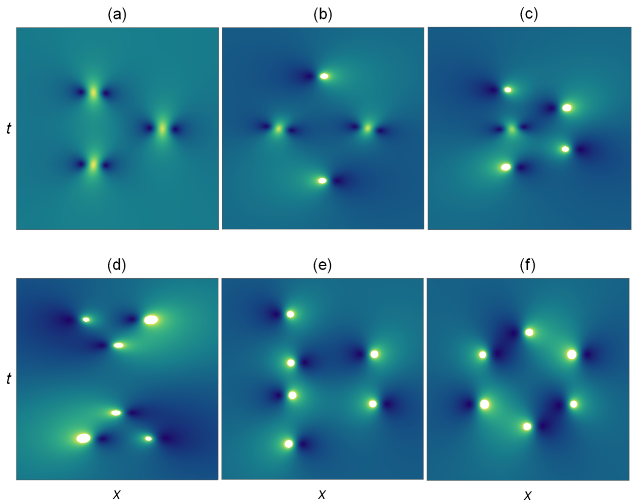

FIG. 3. Six second-order rogue waves (39) with different patterns. (a). $s_0 = \frac{i}{20}; s_1 = 20; s_2 = 0$; (b). $s_0 = 2i; s_1 = 30i$; (c). $s_0 = 2i; s_1 = 10$; (d). $s_0 = 5i; s_1 = 0; s_2 = 0$; (e). $s_0 = 2i; s_1 = 40; s_2 = 0$; (f). $s_0 = 0; s_1 = 30i; s_2 = 0$;

two singular (blowing-up) peaks on the horizontal x axis, and two nonsingular "Peregrine-like" humps on the vertical t axis. In panel (c), these is one "Peregrine-like" nonsingular hump in the middle of two singular peaks on the vertical t axis, plus another two singular peaks locate also on the vertical t axis. The other three panels each contain six singular peaks, which are arranged in different patterns. The maximum number of singular peaks in these solutions is six.

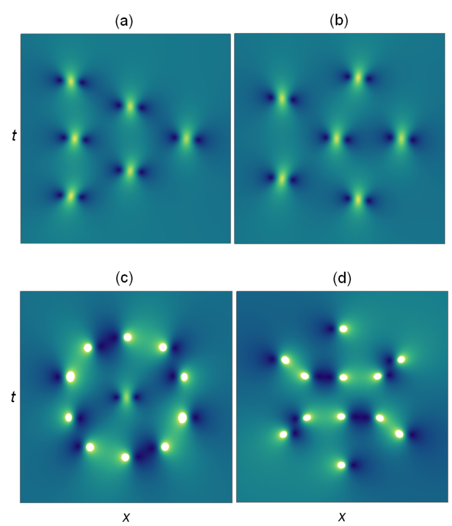

FIG. 4. Four third-order rogue waves (top row: nonsingular solutions; lower row: collapsing solutions). (a). $s_0 = \frac{i}{10}; s_1 = 20; s_2 = 0$ (b). $s_0 = \frac{i}{10}; s_1 = 0; s_2 = -300$; (c). $s_0 = 0; s_1 = 0; s_2 = 300i$; $s_0 = 4i; s_1 = 84; s_2 = 0$; (d). $s_0 = 2i; s_1 = 0; s_2 = 300i$;

Third-order rogue waves would exhibit an even wider variety of solution patterns. Here, four of them are chosen and displayed in Fig. 4. The upper row shows two nonsingular solutions, which contain six "Peregrine-like" humps arranged in triangular and pentagon patterns, resemble those solutions in the local NLS equation[34,35], but not in the $\mathcal{PT}$-symmetric nonlocal NLS equation[20], while the spatial-temporal structures displayed there are different from these two nonsingular patterns.

The lower row in Fig. 4 contains two blowing-up solutions. In panel (c), there is one

"Peregrine-like" nonsingular hump surrounded by ten singular peaks. In panel (d), twelve singular peaks arranging in a very exotic pattern. Again, this maximum number of singular peaks is found to be twelve.

The results given above can be apparently extended to higher order rogue waves. By special choices of the free parameters s_k ($k \in \mathbb{N}^+$), we can yield even richer spatial-temporal patterns, in the form of nonsingular humps, singular peaks or their hybrid patterns, but with more intensity. Moreover, for the fundamental pattern rogue waves(i.e., only s_0 are

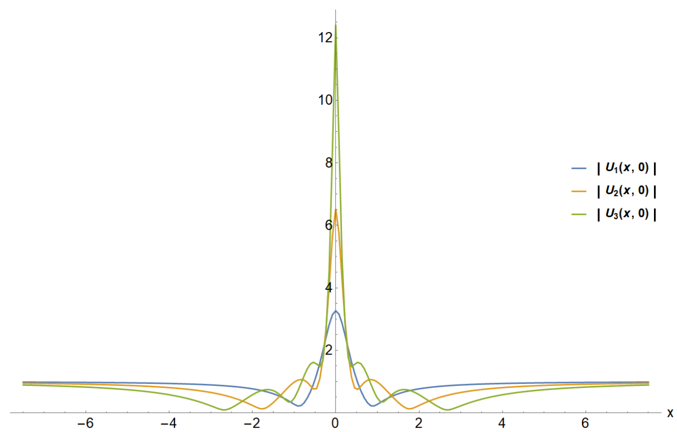

FIG. 5. The 2D plot of $|u_N(x,0)|$ from the first- to the third-order rogue waves, with parameters: $s_0 = \frac{i}{8}; s_1 = 0; s_2 = 0;$

taken as nonzero value while the rest of the parameters are taken as zero.) in the local NLS equation, the central maximum amplitude for each solutions is given by $|u_N(0,0)| = 2N+1$. However, this value becomes higher for nonlocal equation (2). Taking the first to the third order fundamental rogue-wave pattern as an example. It is shown that the elevations for them are numerically attained at $|u_1(0,0)| = 3.26667 > 3$, $|u_2(0,0)| = 6.52338 > 5$, and $|u_3(0,0)| = 12.4318 > 7$ (See Fig.5). Thus, such rogue waves can be fairly dangerous if they arise in physical situations.

III. ROGUE WAVES IN THE REVERSE-TIME NONLOCAL DS SYSTEMS

In this part, we consider rogue waves in the reverse-time nonlocal DS equations, which is recently introduced in refs.[3]. Eqs.(3)-(4) can be regarded as an integrable multidimensional version of the reverse-time nonlocal nonlinear Schrödinger equation.

We start with the following auxiliary linear system:

$$L\Phi = 0, L = \partial_y - J\partial_x - P, \tag{40}$$

$$M\Phi = 0, M = \partial_t - \sum_{j=0}^{2} V_{2-j}\partial^j, \tag{41}$$

$$V_0 = \mathrm{i}\gamma^{-1}J,\ V_1 = \mathrm{i}\gamma^{-1}P,\ V_2 = \frac{\mathrm{i}}{2\gamma}\left(P_x + \gamma^2 J P_y + Q\right),$$

$$J = \gamma^{-1}\begin{pmatrix} 1 & 0 \\ 0 & -1 \end{pmatrix},\ P = \begin{pmatrix} 0 & q \\ -r & 0 \end{pmatrix},\ Q = \begin{pmatrix} \phi_1 & 0 \\ 0 & \phi_2 \end{pmatrix},$$

with,

$$\phi = qr - \frac{1}{2\gamma}(\phi_1 - \phi_2). \tag{42}$$

The compatibility condition $[L, M] = 0$ leads to the following equation:

$$P_t = V_{2,y} - JV_{2,x} - [P, V_2] + \sum_{j=1}^{2} V_{2-j}\partial^j(P), \tag{43}$$

which yields to the following coupled system for potential functions $q(x, y, t)$, $r(x, y, t)$ and $\phi(x, y, t)$:

$$iq_t + \frac{1}{2}\gamma^2 q_{xx} + \frac{1}{2}q_{yy} + (qr - \phi)q = 0, \tag{44}$$

$$\phi_{xx} - \gamma^2\phi_{yy} - 2\,(qr)_{xx} = 0. \tag{45}$$

Then, the reverse-time nonlocal DS equations (3)-(4) are obtained from the above coupled system (44)-(45) under the symmetry reduction:

$$r(x, y, t) = \sigma q(x, y, -t). \tag{46}$$

Under reduction (46), it is noticed that potential matrix P satisfies the following symmetry condition:

$$\tau_\sigma \overline{P}(x, y, t)\tau_\sigma^{-1} = -P^\dagger(x, y, -t), \quad \tau_\sigma = \begin{pmatrix} 1 & 0 \\ 0 & \sigma \end{pmatrix}. \tag{47}$$

Here $^-$ represents the complex conjugation of the function. In this case, we should have $\phi_1(x, y, t) = \phi_1(x, y, -t)$, $\phi_2(x, y, t) = \phi_2(x, y, -t)$. Thus, $\phi(x, y, t)$ is an even-function on t, and $V_2(x, y, t)$ have the property

$$\tau_\sigma \overline{V}_2(x, y, t)\tau_\sigma^{-1} = V_2^\dagger(x, y, -t) + \mathrm{i}\gamma P_x^\dagger(x, y, -t). \tag{48}$$

Afterwards, symmetry conditions (47)-(48) further lead to the symmetry in L and M:

$$\tau_\sigma L^\dagger \tau_\sigma^{-1} = -\overline{L}_{(t\to -t)}, \quad \tau_\sigma M^\dagger \tau_\sigma^{-1} = \overline{M}_{(t\to -t)}. \tag{49}$$

Here, $\dagger$ stands the (formal) adjoint on an operator. Especially, for a matrix A, where $A^\dagger$ denotes the Hermitian conjugate of A.

A. A unified binary Darboux transformstion and its reductions

In this section, we construct the corresponding Darboux transformation in a unified way for the reverse-time nonlocal DSI and DSII equation. It is known that the DT for DSI and DSII equations (local or nonlocal) appears either in the differential form or in the integral form, which are totally different. However, for this reverse-time nonlocal DS system, we can find a unified way to tackle their DTs and represent the solutions in one formula.

The standard scheme for binary DT was firstly introduced by Matveev and Salle.[60] Especially, for operators L and M given in (40)-(41), a binary DT has been constructed,[60,61] which can be written explicitly as

$$G_{\theta,\rho} = I - \theta\Omega^{-1}(\theta, \rho)\partial^{-1}\rho^\dagger, \quad \Omega(\theta, \rho) = \partial^{-1}(\rho^\dagger\theta), \tag{50}$$

where θ satisfy $L(\theta) = 0$, and ρ admits the adjoint operator: $L^\dagger(\rho) = 0$. Then the operator

$$\hat{L} = G_{\theta,\rho} L G_{\theta,\rho}^{-1} \tag{51}$$

can be directly verified to be a new operator which has the same form as L, and so is for $M \to \widehat{M}$. Furthermore, this Darboux transformation makes sense for any $m \times k$ matrices θ and ρ, and we only need $\Omega(\theta, \rho)$ to be an invertible square matrix[61]. By the combination of an elementary DT with its inverse, one derives the Bäcklund transformation between the potential matrices:

$$\hat{P} = P + [J, \theta\Omega^{-1}(\theta, \rho)\rho^\dagger]. \tag{52}$$

Next, to reduce (50) and (52) to the Binary DT for the reverse time nonlocal DS equations (3)-(4), the wave function and the adjoint wave function are restricted to satisfy the following important relation:

$$\rho(x, y, t) = \tau_\sigma \overline{\theta}(x, y, -t). \tag{53}$$

With condition (53), it can be verified that the new potential matrix in (52) indeed preserves the symmetry:

$$\tau_\sigma \overline{\hat{P}}(x, y, t)\tau_\sigma^{-1} = -\hat{P}^\dagger(x, y, -t). \tag{54}$$

At the same time, $\hat{V}_2$ will also preserves symmetry (48) due to (54). Hence new operators $\hat{L}$ and $\hat{M}$ can further satisfy symmetry (49). Therefore, under this reduction, matrix (50) becomes the binary DT for the reverse-time nonlocal DS equations. The Bäcklund transformations (52) for generating new solutions are given as

$$\hat{q} = q + \gamma^{-1}[\theta\Omega^{-1}(\theta, \rho)\rho^\dagger]_{1,2}, \tag{55}$$
$$\hat{\phi} = \phi + 2\gamma^{-2}[\mathbf{tr}(\theta\Omega^{-1}(\theta, \rho)\rho^\dagger)]_x. \tag{56}$$

Taking n different wave-functions θ_i and adjoint wave-functions ρ_i which satisfy reduction (53). Denoting

$$\Theta = (\theta_1, \cdots, \theta_n)\,, \;\mathbf{P} = (\rho_1, \cdots, \rho_n)\,.$$

Introducing $1 \times n$ row vectors ψ_i and φ_i, $i = 1, 2$. The above $2 \times n$ matrices can be further represented by

$$\Theta = \begin{pmatrix} \psi_1 \\ \psi_2 \end{pmatrix}, \quad \mathbf{P} = \begin{pmatrix} \varphi_1 \\ \varphi_2 \end{pmatrix}.$$

Defining the $n \times n$ matrix $\Omega(\Theta, \mathbf{P})$ as:

$$\Omega(\Theta, \mathbf{P}) = \left(\partial^{-1}(\rho_i^\dagger\theta_j)\right)_{1\le i,j\le n}.$$

Hence, the n-fold Bucklünd transformations between potential functions is given as:

$$q_{[n]}(x, y, t) = u_{[0]}(x, y, t) - \frac{2}{\gamma}\frac{\begin{vmatrix} \Omega(\Theta, \mathbf{P}) & \varphi_2^\dagger \\ \psi_1 & 0 \end{vmatrix}}{\det(\Omega(\Theta, \mathbf{P}))}, \tag{57}$$
$$\phi_{[n]}(x, y, t) = w_{[0]}(x, y, t) + 2\gamma^2\partial_x^2\{\log\left[\det\left(\Omega(\Theta, \mathbf{P})\right)\right]\}. \tag{58}$$

This n-fold Bucklünd transformation has been reported[15] by using quasi-determinant technique with simple linear algebra. The proof of expressions (57)-(58) has already been given[15].

B. General binary Darboux transformation

To obtain the high-order solutions, we need to perform the general DT scheme. The idea was firstly introduced by Matveev[60] and further developed by Ling[34] to construct high-order rogue waves in local NLS equation. For this nonlocal DS system, the general binary DT can be also constructed via a direct limitation technique, those are summarised as the following results.

Theorem 3 *The generalized binary Darboux matrix for the reverse time nonlocal DS equations (3)-(4) can be represented as:*

$$G_{[n]} = I - \Theta\Omega^{-1}(\Theta, \mathbf{P})\Omega(\cdot,\; \mathbf{P}),$$

where,

$$
\begin{aligned}
&\theta_i = \theta_i(k_i + \epsilon_i),\ \rho_j = \rho_j(\tilde{k}_j + \tilde{\epsilon}_j),\\
&\widehat{\Theta} = (\Theta_1, \Theta_2, \ldots, \Theta_s),\ \Theta_i = \left(\theta_i^{[0]}, \ldots, \theta_i^{[r_i-1]}\right),\\
&\widehat{\mathbf{P}} = (\mathbf{P}_1, \mathbf{P}_2, \ldots, \mathbf{P}_s),\ \mathbf{P}_j = \left(\rho_j^{[0]}, \ldots, \rho_j^{[r_j-1]}\right),\\
&\Omega(\widehat{\Theta}, \widehat{\mathbf{P}}) = \left(\Omega^{[ij]}\right)_{1\le i,j\le s},\ \Omega^{[ij]} = \left(\Omega^{[ij]}_{m,n}\right)_{r_i\times r_j},\\
&\theta_i = \sum_{k=0}^{r_i-1} \theta_i^{[k]}\epsilon_i^k + \mathcal{O}(\epsilon_i^{r_i}),\ \rho_j = \sum_{k=0}^{r_j-1} \rho_j^{[k]}\tilde{\epsilon}_j^k + \mathcal{O}(\tilde{\epsilon}_j^{r_j}),\\
&\Omega(\theta_j(k_j+\epsilon_j), \rho_i(\tilde{k}_i + \tilde{\epsilon}_i)) = \sum_{m=1}^{r_i}\sum_{m=1}^{r_i} \Omega^{[ij]}_{m,n} + \mathcal{O}(\tilde{\epsilon}_i^{r_i}, \epsilon_j^{r_j}).
\end{aligned}
$$

Moreover, the general Bucklünd transformations between potential functions are given as:

$$
q_{[n]} = q_{[0]} - \frac{2}{\gamma}\frac{\begin{vmatrix} \Omega(\widehat{\Theta}, \widehat{\mathbf{P}}) & \widehat{\mathbf{P}}_2^{\dagger} \\ \widehat{\Theta}_1 & 0 \end{vmatrix}}{\det(\Omega(\widehat{\Theta}, \widehat{\mathbf{P}}))}, \tag{59}
$$

$$
\phi_{[n]} = \phi_{[0]} - 2\partial_x^2\{\log\left[\det\left(\widehat{\Omega}(\Theta, \mathbf{P})\right)\right]\}, \tag{60}
$$

Here, $\widehat{\Theta}_1$ represents the 1-st row of matrix $\widehat{\Theta}$, and $\widehat{\mathbf{P}}_2$ stands the 2-nd row in matrix $\widehat{\mathbf{P}}$.

The proof for above results can be obtained by directly applying the expansions to each matrix element in the n-fold Bucklünd transformation, performing simple determinant operations and taking the limits in (57)-(58).

C. Rogue-wave solutions and their dynamics

It is shown[38,39] that a family of rational solutions were derived by the bilinear method, which generate the rogue waves for the local DS equations. In this work, rogue wave solutions for the reverse time nonlocal DS equations can be constructed via a unified binary Darboux transformation method.

Firstly, choosing a constant $q_{[0]} = c,\ \phi_{[0]} = \sigma c^2\ (c \in \mathbb{R})$ as the seeding solution. Then the eigenfunction solved from Eqs. (40)-(41) has the form

$$
\begin{aligned}
&\xi_i(x,y,t) = c_i \exp\left[\omega_i(x,y,t)\right],\\
&\eta_i(x,y,t) = \frac{\lambda_i c_i}{c}\exp\left[\omega_i(x,y,t)\right],\\
&\omega_i(x,y,t) = \alpha_i x + \beta_i y + \gamma_i t,\ \gamma_i = \mathrm{i}\gamma^{-1}\alpha_i\beta_i,\\
&\alpha_i = -\frac{1}{2}\gamma\left(\lambda_i + \frac{\sigma c^2}{\lambda_i}\right),\ \beta_i = \frac{1}{2}\left(\lambda_i - \frac{\sigma c^2}{\lambda_i}\right),
\end{aligned}
$$

where $\lambda_i = r_i\exp(\mathrm{i}\varphi_i)$, r_i and φ_i are free real parameters, c_i is set to be complex.

Generally, to derive rational type solutions, we choose a more general eigenfunction via superposition principle, which can be written in the form as:

$$
\theta(x,y,t) := \{f_k + \partial_{\varphi_k}\}(\xi_k, \eta_k)^T,\ f_k \in \mathbb{C}. \tag{61}
$$

1. Fundamental rogue waves

To derive the first order rational solution, we set $n = 1$, $c = 1$ with $c_1 = 1$ in formula (57)-(58). Then the first-order rational solution in this reverse-time nonlocal system is:

$$q_1(x,y,t) = 1 - \frac{2F_1(t)}{F(x,y,t)}, \tag{62}$$

$$\phi_1(x,y,t) = \sigma + 2\gamma^2[\ln(F(x,y,t))]_{xx}, \tag{63}$$

where,

$$F_1(t) = 4i\gamma^2(\lambda_1^{-2} + \lambda_1^2)t + 2,\ \ \lambda_1 = r_1 e^{\mathrm{i}\varphi_1},$$
$$F(x,y,t) = \left[\sigma\lambda_1^{-1}(\gamma x + y) - \lambda_1(\gamma x - y) - 2\,\mathrm{i}f_1 + 1\right]^2 + 4\left(\lambda_1^{-2} + \lambda_1^2\right)^2 t^2 + 1.$$

The structure of this rational solution is quite different from that in the partially $\mathcal{PT}$-symmetric nonlocal Davey-Stewartson equations. By analysing the denominator in solution (62), it is shown that this rational solution has different dynamical patterns according to the parameter values of r_1 and φ_1. Those results are discussed separately in the following context.

Reverse-time nonlocal DSI ($\gamma^2 = 1$) equation.

(i). When $\varphi_1 = k\pi$, $\lambda_1 = (-1)^k r_1$ is a real number. In this case, $q_1(x,y,t)$ is a line rogue wave which approaches a constant background, i.e., $q_1 \to 1$, $\phi_1 \to \sigma$ as $t \to \pm\infty$. Defining $m_1 = r_1 - \sigma r_1^{-1}, m_2 = r_1 + \sigma r_1^{-1}$, then $F_1(t)$ and $F(x,y,t)$ becomes:

$$F_1(t) = 2i(m_1^2 + m_2^2)t + 2,$$
$$F(x,y,t) = [H(x,y)]^2 + \left(m_1^2 + m_2^2\right)^2 t^2 + 1,$$
$$H(x,y) = m_1\gamma x - m_2 y + (-1)^k(2\mathrm{i}f_1 - 1).$$

For this solution, if $\mathrm{Re}(f_1) \neq 0$ and $(\mathrm{Re}(f_1))^2 \geq \frac{1}{4}$, then function $F(x,y,t)$ becomes zero at symmetrical critical time $t_c = \pm\frac{\sqrt{4(\mathrm{Re}(f_1))^2-1}}{m_1^2+m_2^2}$, the singularity occurs along on the line:

$$m_1\gamma x - m_2 y - (-1)^k(2\mathrm{Im}(f_1) + 1) = 0$$

in the (x,y) plane.

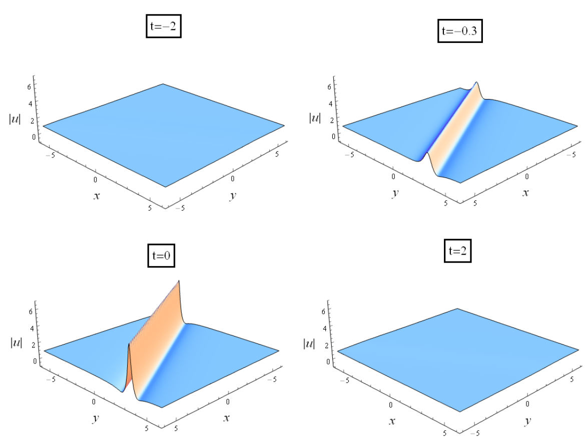

FIG. 6. Fundamental rogue waves in reverse-time nonlocal DS-I equation with parameters: $k = 2$, $\sigma = 1$, $r_1 = 2$, $f_1 = \frac{1}{3}$.

For other choice in the parameter f_1, this solution describes the nonsingular line rogue waves, The imaginary part of f_1 can can be further shifted by x or y. The line in this solution oriented in the $(m_2, \gamma m_1)$ direction of the (x,y) plane. The orientation angle

β of this solution is $\beta = \gamma \arctan(m_1/m_2)$, $(\gamma = \pm 1)$. The width for this line wave is $\sqrt{m_1^2 + m_2^2} = \frac{2}{\sqrt{\sigma \cos 2\beta}}$, so it is angel dependent. Moreover, if $(\mathrm{Re}(f_1))^2 < \frac{1}{4}$, the solution keeps as constant along the line direction with $m_1\gamma x - m_2 y - (-1)^k(2\mathrm{Im}(f_1) + 1) = 0$ fixed. As $t \to \pm\infty$, the solution q uniformly approaches the constant background 1 everywhere in the spatial plane. But in the intermediate times, $|q|$ reaches maximum amplitude $\frac{4(\mathrm{Re}f_1)^2+3}{4(\mathrm{Re}f_1)^2-1}$ (more than three times the background amplitude) at the center of the line wave at time $t = 0$. The speed at which this line approaches its peak amplitude is $\frac{2\sigma}{\cos 2\beta}$, which is also angle dependent. Moreover, as what has been discussed in[38], for a given σ, the line rogue waves in the reverse-time nonlocal DSI equation have a limited range of orientations. When $\sigma = 1$, since r_1 is a real number, one can see that $|m_1/m_2| < 1$, thus the orientation angle of this line rogue wave is between $-45°$ and $45°$. If $\sigma = -1$, the satiation is opposite and the orientation angle is between $45°$ and $135°$. We plot this fundamental line rogue wave in Fig.6 with parameters taken as $k = 2$, $\sigma = 1$, $r_1 = 2$ and $f_1 = \frac{1}{3}$.

Especially, when $\mathrm{Re}(f_1) = 0$, this solution has the property:

$$\overline{q_1}(x, y, t) = q_1(x, y, -t), \tag{64}$$

which indicates that $q_1(x, y, t)$ also admits the local DSI equation.

(ii). When $\varphi_1 = (\frac{2k-1}{2})\pi$, then $\lambda_1 = \mathrm{i}(-1)^{k-1}r_1$ is a purely imaginary number. This generates the rational travelling waves with:

$$\begin{aligned}
&F_1(t) = -2i(m_1^2 + m_2^2)t + 2,\\
&F(x, y, t) = \left(m_1^2 + m_2^2\right)^2 t^2 - [G(x, y)]^2 + 1,\\
&G(x, y) = m_2\gamma x - m_1 y + (-1)^{k-1}(2f_1 + \mathrm{i}).
\end{aligned}$$

The ridge of the solution lays approximately on the following two parallel $[x(t), y(t)]$ trajectories:

$$m_2\gamma x - m_1 y + (-1)^{k-1} 2\mathrm{Re}(f_1) \pm \left(m_1^2 + m_2^2\right) t = 0.$$

Reverse-time nonlocal DSII equation($\gamma^2 = -1$; Here, we take $\gamma = \mathrm{i}$ in the following discussion).

(i). For the first case, if $\sigma = 1$, $r_1 = 1$, i.e., $|\lambda_1| = 1$. We obtain the fundamental line rogue wave. In this case, $q_1(x, y, t)$ approaches a constant background as $t \to \pm\infty$. Defining $m_1 = r_1 - \sigma r_1^{-1}, m_2 = r_1 + \sigma r_1^{-1}$, then $F_1(t)$ and $F(x, y, t)$ becomes:

$$\begin{aligned}
&F_1(t) = -8\mathrm{i}t \cos 2\varphi_1 + 2,\\
&F(x, y, t) = [F_2(x, y)]^2 + 16t^2 \cos^2 2\varphi_1 + 1,\\
&F_2(x, y) = 2x \sin \varphi_1 + 2y \cos \varphi_1 - 2\mathrm{i}f_1 + 1.
\end{aligned}$$

This line rogue wave solution, if $\mathrm{Re}(f_1) \neq 0$ and $(\mathrm{Re}(f_1))^2 \geq \frac{1}{4}$, then function $F(x, y, t)$ becomes zero at symmetrical critical time $t_c = \pm\frac{\sqrt{4(\mathrm{Re}(f_1))^2-1}}{4\cos 2\varphi_1}$. This singularity occurs on the (x, y) plane:

$$2x \sin \varphi_1 + 2y \cos \varphi_1 + 2\mathrm{Im}(f_1) + 1 = 0.$$

For other choice in the parameter f_1, this solution is the nonsingular line rogue wave. The line oriented in the $(\cos \varphi_1, -\sin \varphi_1)$ direction of the spatial plane, the orientation angle is $-\varphi_1$. The width in line rogue wave is angel-independent. For any given time, this solution is a constant along the line with fixed $x \sin \varphi_1 + y \cos \varphi_1$, and approached the constant background 1 with $x \sin \varphi_1 + y \cos \varphi_1 \to \pm\infty$. When $t \to \pm\infty$, the solution q uniformly approaches the constant background 1 everywhere in the spatial plane. In the intermediate times, $|q|$ reaches maximum amplitude $\frac{4(\mathrm{Re}f_1)^2+3}{4(\mathrm{Re}f_1)^2-1}$ (more than three times the background amplitude) at the center of the line wave at time $t = 0$, which is parameter-dependent. This line rogue wave is displayed in Fig.7 with parameters chosen as $\varphi_1 = \frac{\pi}{6}, r_1 = 1, f_1 = \frac{1}{4}$.

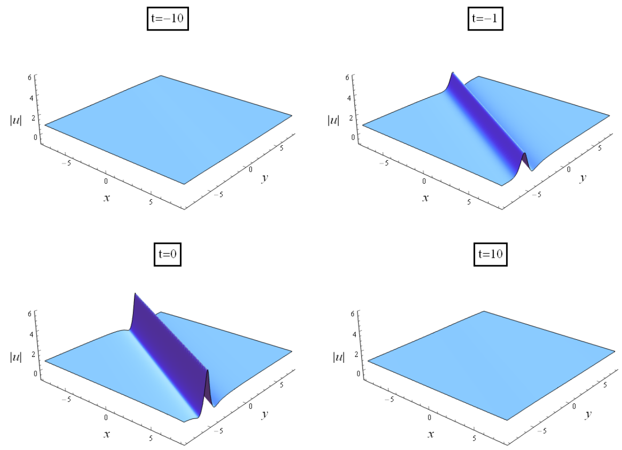

FIG. 7. Fundamental line rogue waves in reverse-time nonlocal DS-II equation with parameters: $\varphi_1 = \frac{\pi}{6}, r_1 = 1, f_1 = \frac{1}{4}$.

It is noted that when $\cos 2\varphi_1 = 0$, this line wave is oriented in $45°$ or $-45°$. In this case, this rational solution is not a rogue wave. Instead, it becomes a stationary line soliton sitting on the constant background. Moreover, when $\mathrm{Re}(f_1) = 0$, this solution also satisfies (64) so that $q_1(x, y, t)$ admits the local DSII equation[39].

(ii). For the second case, if $\sigma = -1$ and $r_1 = 1$, it generates the rational travelling waves with:

$$
\begin{aligned}
F_1(t) &= -8\mathrm{i}t \cos 2\varphi_1 + 2,\\
F(x, y, t) &= -\left[H_1(x, y)\right]^2 + 16t^2 \cos^2 2\varphi_1 + 1,\\
H_1(x, y) &= 2x \cos \varphi_1 - 2y \sin \varphi_1 + 2f_1 + \mathrm{i},
\end{aligned}
$$

and the ridge of the solution lays approximately on the following two parallel $[x(t), y(t)]$ trajectories:

$$2x \cos \varphi_1 - 2y \sin \varphi_1 + 2\mathrm{Re}(f_1) \pm 4t \cos 2\varphi_1 = 0,$$

Noticing that the partially $\mathcal{PT}$-symmetric nonlocal DS system admits the cross-shaped travelling wave solution[20].

2. Muliti rogue waves

One of the important subclass of non-fundamental rogue waves is the multi-rogue waves, which describe the interaction between n individual fundamental rogue waves. These rogue waves are obtained when we take $n > 1$ in rational solution (57)-(58) with n real parameters $r_1, ..., r_n$ or $\varphi_1, ..., \varphi_n$. When $t \to \pm\infty$, the solution (q, ϕ) uniformly approaches the constant background 1 in the entire spatial plane. In the intermediate times, n line rogue waves arise from the constant background, intersect and interact with each other, and then disappear into the background again. For the nonlocal DSI equation, its multi rogue-wave solution consists of n separate line rogue waves in the far field of the spatial plane. However, in the near field, the wavefronts of the rogue wave solution are no longer lines, and there would be some interesting curvy wave patterns. For the nonlocal DSII equation, the multi rogue-waves appear in the form of exploding rogue waves, which develop singularities under suitable choice of parameters.

To demonstrate these multi rogue-wave solutions in the reverse-time nonlocal DS system, we first consider the case of $n = 2$. In this case, two rogue-wave solutions for this reverse-time nonlocal DS system are uniformly contained in only one expression, where λ_1, λ_2, φ_1, φ_2 are free real parameters, f_1, f_2 are free complex parameters.

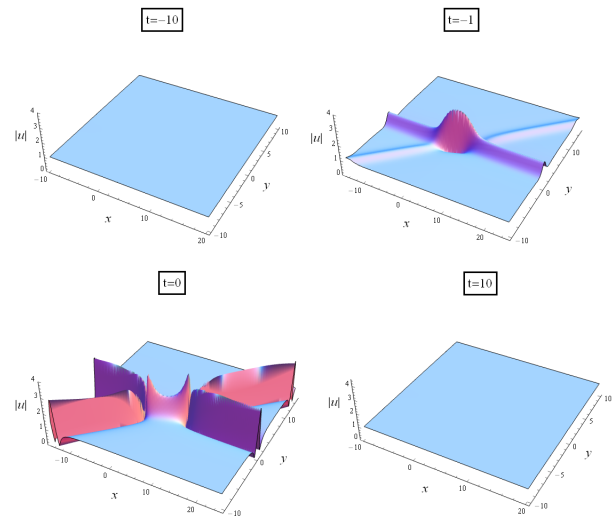

FIG. 8. A two-rogue waves in reverse-time nonlocal DS-I equation with parameters (65).

When $\gamma = 1$, i.e., for the nonlocal DSI equation, a two-rogue-wave solution with parameters

$$\lambda_1 = 1, \quad \lambda_2 = 2, \quad f_1 = 0.05, \quad f_2 = -0.01 \tag{65}$$

is shown in Fig. 8.

Firstly, these two line rogue waves, arising from the constant background, possess higher amplitude in the intersection region at $t = -1$. Afterwards, these higher amplitudes in the intersection region fade, then in the far field, two line rogue solutions rise to higher amplitude at $t = 0$. Afterwards, the solution goes back to the constant background again at large times (see the $t = 10$ panel). During this process, the interaction between two fundamental line rogue waves does not generate very high peaks. Actually, the maximum value of solution $|q|$ does not exceed 4 for all times (i.e., four times the constant background). It is noted that this kind of wave pattern is first found in the local DSI equation[38]. Interestingly, if f_1, f_2 in (65) are purely imaginary numbers, we have $q^*(x, y, t) = q(x, y, -t)$. In that case, this two-rogue-wave solution also admits the local DSI equation.

However, if we choose the value of real parameter r_1 not to be one. For example, if we set

$$\lambda_1 = 1/2, \quad \lambda_2 = 2, \quad f_1 = 0.05, \quad f_2 = -0.01, \tag{66}$$

as what is shown in Fig.9, the maximum value of solution $|q|$ becomes higher and exceeds the value 4, which is different from the previous pattern.

Thus, for larger n, multi-rogue waves in the reverse-time nonlocal DSI equation have qualitatively similar behaviors, more fundamental line rogue waves will arise and interact with each other, and more complicated wave fronts will emerge in the interaction region. For example, with $n = 3$ and parameter choices the corresponding solution is shown in Fig.10.

As can be seen, the transient solution patterns become more complicated. Also, as we could see, wether the maximum value of solution $|q|$ stays below or beyond 4 for all times depends on the choice of the real parameters λ_i. For example, the parameters for Fig.10 are chosen as:

$$\lambda_1 = 1, \ \lambda_2 = 1.5, \ \lambda_3 = 2, \ f_1 = 0.05, \ f_2 = 0, \ f_3 = -0.05. \tag{67}$$

In this case, the transient solution patterns become more complicated. But the maximum value of this solution $|q|$ still stays below 4 in all times. However, if one takes $\lambda_1 = 1/3$ in above parameters, this interaction would be able to create very high amplitude.

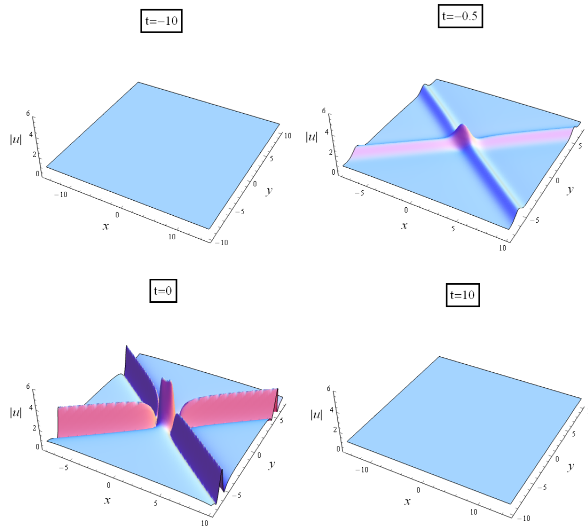

FIG. 9. A two-rogue waves which generate higher amplitude in reverse-time nonlocal DS-I equation with parameters (66).

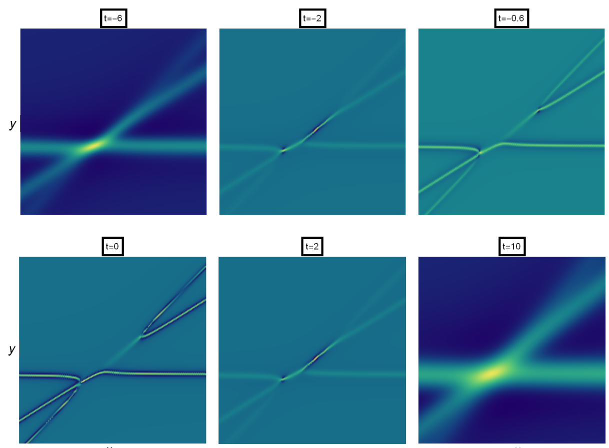

FIG. 10. A three-rogue waves in reverse-time nonlocal DS-I equation with parameters (67).

Next, when $\gamma = 1$, we find some exploding rogue-wave solutions for the reverse-time nonlocal DSII equation. These exploding rogue waves, which arise from the constant background 1, can blow up to infinity in a finite time interval at isolated spatial locations under certain parameter conditions. In this case, the solutions go to a constant background, $q \to 1$, $\phi \to \sigma$, as $t \to -\infty$. To demonstrate, we consider a two-rogue-wave solution whose expression are given by taking $n = 2$ in (57)-(58). Choosing parameters as

$$\lambda_1 = 1, \quad \lambda_2 = \mathrm{i}, \quad f_1 = 0.05, \quad f_2 = 0.025. \tag{68}$$

This exploding rogue-wave solution is displayed in Fig.11.

One can see a cross-shape wave firstly appears in the intermediate times (see the $t = -2.5$, $t = -2$ panels), which describes the nonlinear interaction between two fundamental line rogue waves: one of the line oriented along the x-direction (corresponding to parameter λ_1), the other line oriented along the y-direction (corresponding to parameter λ_2). Afterwards, the peak amplitude in this cross-shape rogue wave becomes much higher instantaneously. In Fig.11, we plotted solution up to time $t = -1.8$, shortly before the blowing-up. One can see the maximum amplitude for this rogue wave solution becomes extremely high.

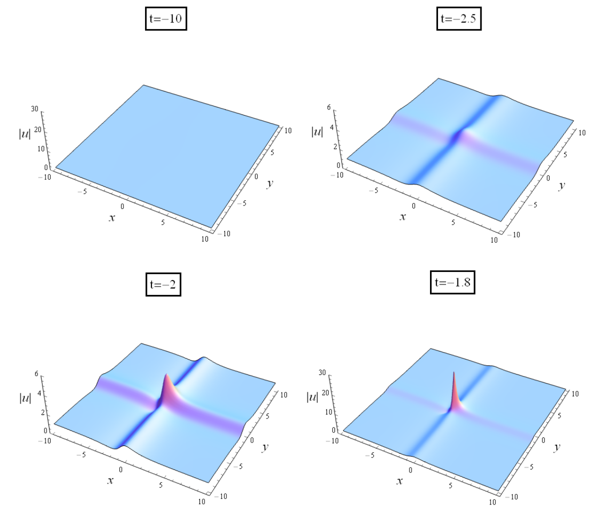

FIG. 11. The exploding rogue waves in reverse-time nonlocal DS-II equation with parameters (68).

For the local DSII equation, multi and higher-order collapsing wave solutions with constant boundary conditions have been derived in[39]. Moreover, for the partially $\mathcal{PT}$-symmetric nonlocal system, similar exploding rogue waves also exist, where the blowups can occur on an entire hyperbola of the spatial plane.

3. High-order rogue waves

Another important subclass of non-fundamental rogue waves is the higher-order rogue waves, which are obtained from the higher-order rational solution with a real value of λ_1. For example, if $n = 2$ in (59)-(60), and we get the second-order rogue-wave solution. To demonstrate these dynamic behaviours, we consider above 2-nd order rogue waves with parameters

$$\gamma = 1, \ \sigma = 1, \ \lambda_1 = 1, \tag{69}$$

while f_1 is a free complex parameter. Thus we get

$$q_1(x, y, t) = \frac{g_1}{h_1}, \tag{70}$$

where $\zeta(y) := y^2 + y + \frac{1}{2}$,

$$h_1 = \left(8t^2 - 2x - 2\zeta\right)^2 + \zeta\left(64t^2 + 4\right) + 4\mathrm{i}f_1\left(2y + 1 - \mathrm{i}f_1\right)\left[-(2y + 1 - \mathrm{i}f_1)^2 - 8t^2 + 2\zeta - 2x - 2\right],$$

$$g_1 = h_1 - 2\left(1 + 4\mathrm{i}t\right)\left[\left(-2\mathrm{i}f_1 + 2y + 1\right)^2 - \left(1 + 4\mathrm{i}t\right)^2 - 4x\right].$$

For solution (70), if f_1 is taken as a purely imaginary number, then denominator function h_1 is real, thus relation (64) is satisfied. However, if f_1 is chosen as real number, then h_1 is complex, in that case, this solution do not satisfy the local DSI equation. By choosing suitable value in f_1, this solution can be nonsingular.

An interesting dynamic behaviour for this solution is that, these higher-order rogue waves do not uniformly approach the constant background as $t \to \pm\infty$. Instead, only parts of their wave structures approaches background as $t \to \pm\infty$. For instance, if we we set $f_1 = 0.05$. When $|t| \gg 1$, this solution becomes a localized lump sitting on the constant background 1 (see the $t = \pm 6$ panels). And this lump disappears as $t \to 0$. At the same time, a parabola-shaped rogue wave generates from the background. Moreover, when $t = 0$, this parabola is approximatively located at

$$x = -y^2 - y - \frac{1}{2}.$$

Visually, the solution displayed in Fig.12 can be described as an incoming lump being reflected back by the appearance of a parabola-shaped rogue wave. This interesting pattern is firstly obtained via the bilinear method in ref[38]. It is indeed surprising that a similar pattern can be produced in this reverse-time nonlocal DSI equation, although the expression for this solution can be different.

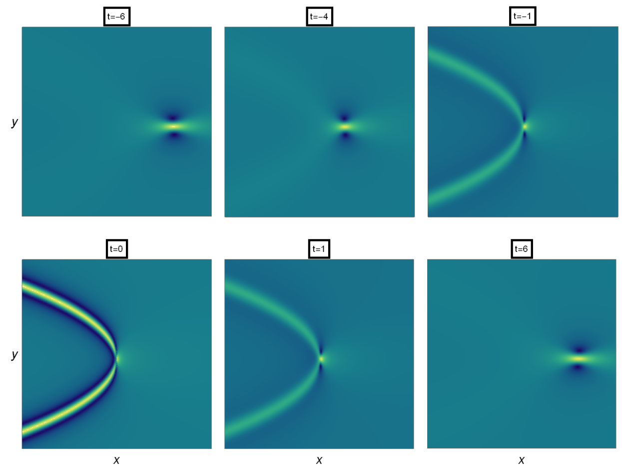

FIG. 12. The second order rogue waves in reverse-time nonlocal DS-I equation with parameters (69).

However, when $\gamma^2 = -1$, we only derive some higher-order rational solutions with almost full-time singularities. Hence, it is still unknown whether there exists nonsingular or finite-time blowing-up high-order rogue waves in the reverse time nonlocal DS-II equation.

IV. SUMMARY AND DISCUSSION

In this article, general rogue waves have been derived for the reverse time nonlocal NLS equation (2) and the reverse time nonlocal DSI and DSII equations (3)-(4) by Darboux transformation method under certain symmetry reductions. It is interesting to show that a new unified binary DT has been constructed for this reverse time nonlocal DS system. Thus, the rogue-wave solution in reverse time nonlocal DSI and DSII equation can be written in a unified formula.

New dynamics of rogue waves is further explored. It is shown the (1+1)-dimensional fundamental rogue waves can be bounded for both x and t, or develop collapsing singularities. It is also shown that the (1+2)-dimensional fundamental line rogue waves can be bounded for all space and time, or have finite-time blowing-ups. All these types depend on the values of free parameters contained in the solution. In addition, the dynamics patterns in the multi- and higher-order rogue waves exhibits richer structures, most of which are found in the nonlocal integrable equations for the first time. For example, the (1+1)-dimensional higher-order rogue waves exhibit more hybrid of collapsing and non-collapsing peaks, arranging in triangular, pentagon, circular and other erotic patterns. The (1+2)-dimensional multi-rogue waves describe the interactions between several fundamental line rogue waves, and some curvy wave patterns with higher amplitudes appear due to the interaction. However, for the (1+2)-dimensional higher-order rogue waves, only part of the wave structure rises from the constant background and then retreats back to it, which possesses the parabolas-like shapes. While the other part of the wave structure comes from far distance as a localized lump, which interacts with the rogue waves in the near field and then reflects back to the large distance again. These rogue-wave to the nonlocal equations generalize the rogue waves of the local equation into the reverse-time satiation, which could play a role in the physical understanding of rogue water waves in the ocean. In addition, the DT reduction method in our paper can be generalized to look for rogue waves in other types of integrable nonlocal equations, for example, the reverse-space, or the reverse-space-time nonlocal equations[3].

ACKNOWLEDGMENT

This project is supported by the National Natural Science Foundation of China (No.11675054 and 11435005), Global Change Research Program of China (No.2015CB953904), and Shanghai Collaborative Innovation Center of Trustworthy Software for Internet of Things (No. ZF1213).

[1] M. J. Ablowitz and Z. H. Musslimani, “Integrable nonlocal nonlinear Schrödinger equation”, Phys. Rev. Lett. 110, 064105 (2013).
[2] M. J. Ablowitz and Z. H. Musslimani, “Integrable discrete $\mathcal{PT}$-symmetric model”, Phys. Rev. E 90, 032912 (2014).
[3] M.J. Ablowitz and Z.H. Musslimani, “Integrable nonlocal nonlinear equations”, Stud. Appl. Math. DOI: 10.1111/sapm.12153 (2016).
[4] Z. Yan, “Integrable $\mathcal{PT}$-symmetric local and nonlocal vector nonlinear Schrödinger equations: A unified two-parameter model,” Appl. Math. Lett. 47, 61–68 (2015).
[5] A. Khara and A. Saxena, “Periodic and hyperbolic soliton solutions of a number of nonlocal nonlinear equations”, J. Math. Phys. 56, 032104 (2015).
[6] M.J. Ablowitz and Z.H. Musslimani, “Inverse scattering transform for the integrable nonlocal nonlinear Schrödinger equation,” Nonlinearity 29, 915–946 (2016).
[7] C Song, D. Xiao and Z. Zhu ”Reverse Space-Time Nonlocal Sasa-Satsuma Equation and Its Solutions.” Journal of the Physical Society of Japan 86(2017).
[8] B. Yang and J. Yang, “Transformations between nonlocal and local integrable equations”, Stud. Appl. Math. DOI: 10.1111/sapm.12195 (2017).
[9] A.S. Fokas, “Integrable multidimensional versions of the nonlocal nonlinear Schrödinger equation”, Nonlinearity 29, 319–324 (2016).
[10] S.Y. Lou, “Alice-Bob systems, P_s-T_d-C principles and multi-soliton solutions”, https://arxiv.org/abs/1603.03975 (2016).
[11] S.Y. Lou and F. Huang, “Alice-Bob physics: coherent solutions of nonlocal KdV systems”, Scientific Reports 7, 869 (2017).
[12] Z.X. Zhou, “Darboux transformations and global solutions for a nonlocal derivative nonlinear Schrödinger equation”, arXiv:1612.04892 [nlin.SI] (2016).
[13] Z.X. Zhou, “Darboux transformations and global explicit solutions for nonlocal Davey-Stewartson I equation”, arXiv:1612.05689 [nlin.SI] (2016).
[14] J.G. Rao, Y. Cheng and J.S. He, “Rational and semi-rational solutions of the nonlocal Davey-Stewartson equations”, Stud. Appl. Math. 139, 568–598 (2017).
[15] B. Yang and Y. Chen, “Dynamics of Rogue Waves in the Partially $\mathcal{PT}$-symmetric Nonlocal Davey-Stewartson Systems”, arXiv:1710.07061 [math-ph] (2017).
[16] C.Q. Song, D.M. Xiao and Z.N. Zhu, “Solitons and dynamics for a general integrable nonlocal coupled nonlinear Schrödinger equation”, Commun. Nonlinear Sci. Numer. Simul. 45, 13–28 (2017).
[17] J.L. Ji and Z.N. Zhu, “On a nonlocal modified Korteweg-de Vries equation: integrability, Darboux transformation and soliton solutions”, Commun. Nonlinear Sci. Numer. Simul. 42 699–708 (2017).
[18] V. S. Gerdjikov and A. Saxena, “Complete integrability of nonlocal nonlinear Schrödinger equation”, J. Math. Phys. 58, 013502 (2017).
[19] M.J. Ablowitz, X. Luo, and Z.H. Musslimani, “Inverse scattering transform for the nonlocal nonlinear Schrödinger equation with nonzero boundary conditions”, arXiv:1612.02726 [nlin.SI] (2016).
[20] B. Yang and J. Yang, ”General rogue waves in the $\mathcal{PT}$-symmetric nonlinear Schrödinger equation”, arXiv:1711.05930 [nlin.SI] (2017).
[21] S.V. Suchkov, A.A. Sukhorukov, J. Huang, S.V. Dmitriev, C. Lee and Y.S. Kivshar, “Nonlinear switching and solitons in $\mathcal{PT}$-symmetric photonic systems”, Laser Photonics Rev. 10, 177 (2016).
[22] V.V. Konotop, J. Yang and D.A. Zezyulin, “Nonlinear waves in $\mathcal{PT}$-symmetric systems,” Rev. Mod. Phys. 88, 035002 (2016).
[23] T.A. Gadzhimuradov and A.M. Agalarov, “Towards a gauge-equivalent magnetic structure of the nonlocal nonlinear Schrödinger equation”, Phys. Rev. A 93, 062124 (2016).
[24] A. Beygi, S. P. Klevansky and C. M. Bender, “Coupled oscillator systems having partial PT symmetry”, Phys. Rev. A 91, 062101 (2015).
[25] Y. V. Kartashov, V. V. Konotop and L. Torner, “Topological states in partially-PT-symmetric azimuthal potentials,” Phys. Rev. Lett 115, 193902 (2015).
[26] C. Kharif, E. Pelinovsky and A. Slunyaev, *Rogue Waves in the Ocean* (Springer, Berlin, 2009)
[27] D. R. Solli, C. Ropers, P. Koonath and B. Jalali, “Optical rogue waves,” 2007 Nature 450, 1054–1057.

[28]D. H. Peregrine, "Water waves, nonlinear Schrodinger equations and their solutions", 1983 J. Aust. Math. Soc. B 25, 16–43.
[29]N. Akhmediev, A. Ankiewicz and M. Taki, "Waves that appear from nowhere and disappear without a trace", Phys. Lett. A 373, 675–678 (2009).
[30]N. Akhmediev, A. Ankiewicz, J. M. Soto-Crespo, "Rogue waves and rational solutions of the nonlinear Schrodinger equation," 2009 Physical Review E 80, 026601.
[31]A. Ankiewicz, P. A. Clarkson, N. Akhmediev. "Rogue waves, rational solutions, the patterns of their zeros and integral relations," 2010 J. Phys. A 43, 122002.
[32]P. Dubard, P. Gaillard, C. Klein and V. B. Matveev, "On multi-rogue wave solutions of the NLS equation and positon solutions of the KdV equation", 2010 Eur. Phys. J. Spec. Top. 185, 247–58.
[33]P. Dubard and V. B. Matveev, "Multi-rogue waves solutions to the focusing NLS equation and the KP-I equation", 2011 Nat. Hazards Earth Syst. Sci. 11, 667–72.
[34]B. L. Guo, L. M. Ling and Q. P. Liu, "Nonlinear Schrodinger equation: generalized Darboux transformation and rogue wave solutions," 2012 Phys. Rev. E 85, 026607.
[35]Y. Ohta and J. Yang, "General high-order rogue waves and their dynamics in the nonlinear Schrodinger equation", 2012 Proc. R. Soc. Lond. A 468, 1716–1740.
[36]S. Xu, J. He and L. Wang, "The Darboux transformation of the derivative nonlinear Schrödinger equation," 2011 J. Phys. A 44, 305203.
[37]F. Baronio, M. Conforti, A. Degasperis and S. Lombardo, "Rogue waves emerging from the resonant interaction of three waves," 2013 Phys. Rev. Lett. 111, 114101.
[38]Y. Ohta and J. Yang, "Rogue waves in the Davey-Stewartson I equation", 2012 Phys. Rev. E 86, 036604.
[39]Y. Ohta and J. Yang, "Dynamics of rogue waves in the Davey-Stewartson II equation", 2013 J. Phys. A 46, 105202.
[40]A. Ankiewicz, N. Akhmediev and J. M. Soto-Crespo "Discrete rogue waves of the Ablowitz- Ladik and Hirota equations," 2010 Phys. Rev. E 82, 026602.
[41]Y. Ohta and J. Yang, "General rogue waves in the focusing and defocusing Ablowitz-Ladik equations", 2014 J. Phys. A 47, 255201.
[42]A. Ankiewicz, J. M. Soto-Crespo and N. Akhmediev, "Rogue waves and rational solutions of the Hirota equation", 2010 Phys. Rev. E 81, 046602.
[43]Y. S Tao and J. S. He, "Multisolitons, breathers, and rogue waves for the Hirota equation generated by the Darboux transformation", 2012 Phys. Rev. E 85, 026601.
[44]F. Baronio, A. Degasperis, M. Conforti and S. Wabnitz, "Solutions of the vector nonlinear Schrödinger equations: evidence for deterministic rogue waves," 2012 Phys. Rev. Lett. 109, 044102.
[45]N. V. Priya, M. Senthilvelan and M. Lakshmanan, "Akhmediev breathers, Ma solitons, and general breathers from rogue waves: a case study in the Manakov system," 2013 Phys. Rev. E 88, 022918.
[46]G. Mu, Z. Qin and R. Grimshaw, "Dynamics of rogue waves on a multi-soliton background in a vector nonlinear Schrödinger equation", SIAM J. Appl. Math. 75 (1), (2015).
[47]G. Mu and Z. Qin, "Dynamic patterns of high-order rogue waves for Sasa-Satsuma equation," 2016 Nonlinear Anal. Real World Appl. 31, 179–209.
[48]L. Ling, "The algebraic representation for high order solution of Sasa-Satsuma equation," 2016 Discrete Continuous Dyn Syst Ser B 9, 1975–2010.
[49]L. M. Ling, B. F. Feng and Z. Zhu, "Multi-soliton, multi-breather and higher order rogue wave solutions to the complex short pulse equation," 2016 Physica D 327, 13–29.
[50]X. Wang, Y. Li, F. Huang and Y. Chen, "Rogue wave solutions of AB system", Commun. Nonlinear Sci. Numer. Simulat. 20 (2015) 434–442
[51]J. Chen, Y. Chen, B. F. Feng, Y. Ohta "General high-order rogue waves of the (1+1)-dimensional Yajima-Oikawa system", arXiv:1709.03781 [nlin.SI](2017).
[52]X. Zhang and Y. Chen, "Deformation rogue wave to the (2+1)-dimensional KdV equation", Nonliear Dyn. 90 (2017) 755–763
[53]J. Yang, "General N-solitons and their dynamics in several nonlocal nonlinear Schrödinger equations", arXiv:1712.01181 [nlin.SI](2017).
[54]M.J. Ablowitz and H. Segur 1981 *Solitons and Inverse Scattering Transform* (SIAM, Philadelphia).
[55]S. Novikov, S.V. Manakov, L.P. Pitaevskii and V.E. Zakharov 1984 *Theory of Solitons* (Plenum, New York)
[56]J. Yang, *Nonlinear Waves in Integrable and Non integrable Systems* (SIAM, Philadelphia, 2010).
[57]D. Bian, B. L. Guo and L. M. Ling. "High-Order Soliton Solution of Landau-Lifshitz Equation," 2015 Stud. Appl. Math. 134, 181–214.
[58]M. Manas, "Darboux transformations for the nonlinear Schrodinger equations," 1996 Journal of Physics A: Mathematical and General 29, 7721.
[59]J.L. Cieslinski, "Algebraic construction of the Darboux matrix revisited", J. Phys. A 42, 404003 (2009).
[60]M. A. Salle and V. B. Matveev. "Darboux transformations and solitons." (Springer-Verlag, Berlin, 1991)
[61]J. J. C. Nimmo, C. R. Gilson and Y. Ohta, "Applications of Darboux transformations to the self-dual Yang-Mills equations", Theor. Math. Phys. 122, 239–246 (2000).